

UNCLASSIFIED

Defense Technical Information Center
Compilation Part Notice

ADP013685

TITLE: Measurement and 3D Computer Simulation of the Crystallinity
Distribution in Injection Molded Syndiotactic Polystyrene

DISTRIBUTION: Approved for public release, distribution unlimited

This paper is part of the following report:

TITLE: DNS/LES Progress and Challenges. Proceedings of the Third
AFOSR International Conference on DNS/LES

To order the complete compilation report, use: ADA412801

The component part is provided here to allow users access to individually authored sections of proceedings, annals, symposia, etc. However, the component should be considered within the context of the overall compilation report and not as a stand-alone technical report.

The following component part numbers comprise the compilation report:

ADP013620 thru ADP013707

UNCLASSIFIED

MEASUREMENT AND 3D COMPUTER SIMULATION OF THE CRYSTALLINITY DISTRIBUTION IN INJECTION MOLDED SYNDIOTACTIC POLYSTYRENE

RICHARD D. SUDDUTH, PAVAN K. YARALA

Department of Chemical Engineering

University of Louisiana at Lafayette, Lafayette, LA 70504-4130

QIN SHENG

Department of Mathematics

University of Dayton, Dayton, OH 45469-2316

KEVIN NICHOLS

Dow Chemical Company, Midland, MI 48667

Abstract

Injection molding of semi-crystalline polymers has been one of the most important yet complicated fabrication processes that combines polymer rheology, heat transfer, and crystallization kinetics. 3D mathematical modeling of polymer flow, and computer simulation of distributions of crystallinity in a semi-crystalline polymer in injection molding applications were studied in this project. Our modeling includes the shear stress and thermal conduction in the width direction and will also eventually provide details of the polymer flow in intricate small cavities of changing cross sections. The simulation developed in this study predicted 3D crystallization properties of syndiotactic polystyrene as a function of position in an injection molded part. The predicted crystallinity distributions were effectively described across a profile at various locations along the flex bar as a function of different molding temperatures and different hold times.

1. Introduction

Computer simulations of injection molding of semicrystalline polymer components have been an active area of research⁽¹⁻⁶⁾. The primary goal of this project was to develop 3D computer simulated virtual integrated prototyping (VIP), rather than traditional 2D Hele-Shaw approximations or smaller scale physical trials, to enhance downstream plastics manufacturing-particularly injection molding. Primary semi-crystalline polymers evaluated include polyphenylene sulfide and syndiotactic polystyrene. Preliminary results from this study have been presented and published elsewhere⁽⁷⁻⁹⁾. Several other authors have also published simulation results⁽¹⁰⁻¹²⁾. The simulation results in this study have focused almost exclusively on syndiotactic polystyrene (244,000 Mol. Wt.). The confirmation of our model also involved the

evaluation of injection-molded parts made from syndiotactic polystyrene. The predicted crystallinity distributions were compared with measured values from molded parts.

2. Governing Equations

Let L , W , H be the length, width and thickness of a slit mold region, respectively. We consider the following mass, momentum and energy balance equations:

$$Q = \int_0^W \int_0^H u dy dx \quad (1)$$

$$0 = \frac{\partial}{\partial y} \left(\eta \frac{\partial u}{\partial y} \right) + \frac{\partial}{\partial z} \left(\eta \frac{\partial u}{\partial z} \right) - \frac{\partial P}{\partial x} \quad (2)$$

$$\rho C_p \left(\frac{\partial T}{\partial t} + u \frac{\partial T}{\partial x} \right) = k \frac{\partial^2 T}{\partial y^2} + k \frac{\partial^2 T}{\partial z^2} + \eta \dot{\gamma}^2 \quad (3)$$

where the heat capacity, C_p , is

$$C_p = C_p' - \lambda_{\infty} \frac{dX}{dT} \quad (4)$$

and u , P , T , k , ρ , C_p , λ_{∞} , X , η , $\dot{\gamma}$ are velocity, pressure, temperature, thermal conductivity, density, specific heat, heat of crystallization, fraction of crystallinity, viscosity and shear rate, respectively.

Many applications in injection molding require processing polymers at temperatures below the glass transition temperature, T_g , and at temperatures over the melting point, T_m . We propose a new model^(13,14) that allows appropriate crystallization results to be obtained over the entire temperature range of processing:

$$\text{Log}_{10}(-\text{Log}_{10} k(T)) = \text{Log}_{10}(-\text{Log}_{10} k_p) + aY + bY^2 + cY^3 + dY^4 + eY^5 + fY^6 \quad (5)$$

where $Y = (T - T_p)^2$, $k(T)$ is the crystallization rate at processing temperature T , k_p is the peak crystallization rate constant, a , b , c , d , e and f are numeric constants and T_p is the peak crystallization temperature.

The sensitivity of k_p and T_p to shear stress, τ , is shown by the following⁽¹⁵⁾:

$$T_p = T_{pq} + E_{STK}(\tau), \quad \text{Log}_{10} k_p = \text{Log}_{10} k_{pq} + E_{SK}(\tau) \quad (6)$$

Since the shear stress constants E_{SK} and E_{STK} for syndiotactic polystyrene were not available for this study, they were assumed to be comparable to those by Hsiung⁽¹⁵⁾ for polyphenylene sulfide based on the data of Haas, et al⁽¹⁶⁾. On the other hand, the true induction time evaluated must be generated from an equation introduced by Sifleet et al⁽¹⁷⁾.

In our study, the induction time was determined using the following model:

$$t_i = t_{ib} e^{C_{ii}(T - T_{ib})^2} \quad (7)$$

The effect of shear stress, τ , on the induction time was again addressed from the expressions proposed by Hsuing⁽¹⁵⁾ for polyphenylene sulfide as:

$$T_b = T_{bq} + E_{STi}(\tau), \quad \text{Log}_{10} t_{ib} = \text{log}_{10} t_{ibq} - E_{Sti}(\tau) \quad (8)$$

Values of the constants for E_{STi} and E_{Sti} were evaluated from the data of Hsuing⁽¹⁵⁾ and related studies^(16,18-20) for polyphenylene sulfide.

The melt viscosity, η , of the syndiotactic polystyrene was evaluated using the Cross law⁽²¹⁾ as a function of shear rate (see Verhoyen et al⁽²²⁾).

2.1. Fractional Crystallinity System of Integro-Differential Equations

It was known^(8,9) that the following system was satisfied by the fractional crystallinity,

$$\frac{\partial X}{\partial t} = \exp(-I^{n_c}) n_c I^{(n_c-1)} [K(x, y, t) - K(x, y, t_{cs})] \quad (9)$$

$$\frac{\partial X}{\partial x} = \exp(-I^{n_c}) n_c I^{(n_c-1)} \left[\int_{t_{cs}}^t \left(\frac{\partial K}{\partial T} \frac{\partial T}{\partial x} + \frac{\partial K}{\partial \tau} \frac{\partial \tau}{\partial x} \right) dt \right] \quad (10)$$

where

$$I = \int_{t_{cs}}^t K(T(x, y, t), \tau(x, y, t)) dt$$

Initial polymer melt temperature T_o was taken as the polymer processing temperature at the shutoff nozzle. It was observed that the degradation of syndiotactic polystyrene is considerably lower if the temperatures were kept below 305°C. The melt temperature was taken to be 305°C. $T_o = 305^\circ\text{C}$ while wall temperature, T_w , is a constant.

$$T(x, H, z, t) = T(x, 0, z, t) = T(x, y, W, t) = T(x, y, 0, t) = T_w \quad (11)$$

The following homogeneous velocity on the boundaries of the mold was considered.

$$u(x, H, z, t) = u(x, 0, z, t) = u(x, y, W, t) = u(x, y, 0, t) = 0.0 \quad (12)$$

The melt front of the polymer was considered to be flat and the temperature was assumed to be uniform all over the melt front. The uniform temperature is equal to the centerline temperature at the stream-wise location immediately upstream of the melt front. The curvature and the transverse flows associated with the melt front due to the fountain flow effect were neglected. Thus we have the following equality:

$$T(x_{mf}, y, z, t) = T\left(x_{mf} - \Delta x, \frac{1}{2H}, \frac{1}{2W}, t\right) \quad (13)$$

2.2. Numerical Method

Introduction of the discrete parameters, Δx , Δy , Δz and Δt along x , y , z (i , j , k) direction s and time, $t(n)$, into the energy balance equation yields the following implicit schemes via the parallel splitting algorithm^(8,9,23).

$$\begin{aligned} -\frac{u_{(i,j,k)}^n}{\rho C_p} \frac{1}{\Delta x} T_{1(i-1,j,k)}^{n+1} + \left(\frac{1}{\Delta t} + \frac{u_{(i,j,k)}^n}{\rho C_p} \frac{1}{\Delta x} \right) T_{1(i,j,k)}^{n+1} &= \frac{1}{\Delta t} T_{1(i,j,k)}^n + \frac{\eta \dot{\gamma}^2}{\rho C_p} + C \\ -\frac{k}{\rho C_p} \frac{1}{\Delta y^2} T_{2(i,j-1,k)}^{n+1} + \left(\frac{1}{\Delta t} + \frac{2k}{\rho C_p \Delta y^2} \right) T_{2(i,j,k)}^{n+1} - \frac{k}{\rho C_p} \frac{1}{\Delta y^2} T_{2(i,j+1,k)}^{n+1} &= \frac{1}{\Delta t} T_{2(i,j,k)}^n \\ -\frac{k}{\rho C_p} \frac{1}{\Delta z^2} T_{3(i,j,k-1)}^{n+1} + \left(\frac{1}{\Delta t} + \frac{2k}{\rho C_p \Delta z^2} \right) T_{3(i,j,k)}^{n+1} - \frac{k}{\rho C_p} \frac{1}{\Delta z^2} T_{3(i,j,k+1)}^{n+1} &= \frac{1}{\Delta t} T_{3(i,j,k)}^n \end{aligned}$$

$$\begin{aligned} C &= \frac{|f_c \lambda_\infty|}{C_p} \{ \exp(-I^{n_c}) n_c I^{(n_c-1)} [K(x,y,t) - K(x,y,t_{cs})] + \\ &u_{(i,j,k)}^n (\exp(-I^{n_c}) n_c I^{(n_c-1)} \left[\int_{t_{cs}}^t \left(\frac{\partial K}{\partial T} \frac{\partial T}{\partial x} + \frac{\partial K}{\partial \tau} \frac{\partial \tau}{\partial x} \right) dt \right] \} \end{aligned}$$

Thus, by applying the parallel splitting algorithm⁽²³⁾, the solution of the energy balance equation can be obtained with a neglectful error as

$$\begin{aligned} T^{n+1} &= 1/2(\exp\{\Delta t M_1\} \exp\{\Delta t M_2\} \exp\{\Delta t M_3\} + \\ &\exp\{\Delta t M_3\} \exp\{\Delta t M_2\} \exp\{\Delta t M_1\}) T^n \end{aligned} \quad (14)$$

where M_1 , M_2 and M_3 are tri-diagonal matrices generated.

4. Computer Program Simulation Results

4.1. Simulation of Crystallinity Distributions at Different Holding Times and Different Locations

Computer simulated crystallinity distributions at a mold temperature of 200°C and an injection speed of 23.2 cc/sec at Location #1 in Figure 1 are summarized in Figures 2 as a function of holding time. In all the figures plotted from the simulation results the direction shown as Z direction corresponds to width (1/2 in) of the sample and the direction shown as Y direction corresponds to thickness (1/8 in) of the sample. The location indicated as 'entrance' is located near the gate and the location indicated, as Location #3 is located further down the sample along the direction of flow. The third axis in the figures shows the magnitude of the fraction of crystallinity, X , developed. The value of $X = 1$ along this axis direction indicates

the maximum crystallinity that can develop at any point. The maximum corresponded to a heat of fusion which was approximately 61.7 percent of the maximum crystallinity possible or $f_c = .617$ giving: $|f_c \lambda_\infty| = .617$ (53.2 Joules/gram) = 32.82 Joules/gram.

As shown elsewhere^(13,14), the maximum crystallization rate for the syndiotactic polystyrene utilized in this study can be achieved at a temperature of approximately 200°C. A rapid surface crystallinity development at 200°C is indicated in Figure 2 as a function of holding time at location #1. The computer simulated crystallinity at a mold temperature of 200°C and an injection speed of 23.2 cc/sec is also indicated at several different locations in Figure 3 at a holding time of 60 sec.

4.2. Crystallinity Distribution at Two Locations as a Function of Mold Temperature at a Given Holding Time and a Specific Injection Speed

The injection molding we considered was at mold temperatures of 50°C, 90°C, 150°C and 190°C and an injection speed of 23.2 cc/sec. The simulations for these runs are indicated in Figure 4 for location position indicated in Figure 1 as the entrance. Assuming that the mass forming the injection molded polymer bar remained the same independent of the temperature of the mold, then the old mold temperature and new estimated mold temperatures were as follows:

$T_{MOLD}, ^\circ C$	$T_{NEW}, ^\circ C$
50°C	132.3 (135)
90°C	159.4 (160)
150°C	200 (200)
190°C	227.1 (230)

The new computer injection molding simulations for mold temperatures of 135°C, 160°C, 200°C and 230°C are indicated in Figures 5 at the entrance location.

5. Experimental

The syndiotactic polystyrene used in this study was supplied by the Dow Chemical Company and had a molecular weight currently characteristic of the production grade of syndiotactic polystyrene (Mol.wt = 244,000). Most of the experimental details for the crystallinity and injection molding measurements have been reported elsewhere^(13,14). The crystallinity measurements determined at four different mold temperatures (50°C, 90°C, 150°C and 190°C) are summarized in Figures 6 and 7.

Since the maximum crystallization rate was found to occur at approximately 200°C, it was expected that the mold temperature of 190°C would have given the maximum amount of surface crystallinity. However, the maximum surface crystallinity was achieved with a mold temperature of 150°C instead of 190°C. This result strongly suggested that the effective mold temperature at 150°C was probably

nearer to the 200°C as proposed in an earlier section. Comparison of these experimental results with the simulated results in Figures 4 & 5 would also be consistent with this observation.

6. Conclusion

In this study, four mold temperatures (50°C, 90°C, 150°C and 190°C) were experimentally evaluated and compared with computer-simulated results. For the injection molded bar simulated in this study it was found that the maximum crystallinity characteristic of a theoretical mold temperature of approximately 200°C was experimentally achieved at a mold temperature of approximately 150°C at an injection speed of 23.3 cc/min. Using a correction factor approach and local heating it was found that the thermal transfer of energy apparently allows a temperature of approximately 200°C to be achieved in the mold at a mold temperature of 150°C.

By addressing effective computer simulation and appropriate experimental outputs for syndiotactic polystyrene, it has been shown that an optimized control of the injection molding process can be developed for better commercial applications.

Acknowledgements

The Authors gratefully acknowledge the support of this project through grants from the Louisiana Board of Regents and Dow Chemical Company. R. Dugyala significantly contributed to the computer programming in the study as a graduate student in chemical engineering. The authors also acknowledge important support from H. Spence of Ash Industries in preparing injection-molding samples evaluated.

References

1. AI Isayev, Y. Churdant and X. Guo (2000) Comparative study of Ziegler-Natta and metallocene based polypropylene in injection molding – simulation and experiment, *Inter. Polymer Processing*, Vol.15, pp. 72-82
2. X. Guo and AI Isayev (2000) Residual stresses and birefringence in injection molding of semicrystalline polymer- Part II: experiment and simulations, *Inter. Polymer Processing*, Vol.14, pp. 387-398
3. S. C. Chen, Y. C. Chen and H. S. Peng (2000) Simulation of injection-compression-molding process. Part II: influence of process characterization on part shrinkage, *J. Appl. Polymer Sci.*, Vol.75, pp. 1640-1654
4. X. Guo, AI Isayev and L. Guo (1999) Crystallinity and microstructure in injection moldings of isotactic polypropylenes. Part I: a new approach to modeling and model parameters, *Polymer Eng. Sci.*, Vol.39, pp. 2096-2114
5. X. Guo, AI Isayev and M. Demiray (1999) Crystallinity and microstructure in injection moldings of isotactic polypropylenes. Part II: simulation and experiment, *Polymer Eng. Sci.* Vol.39, pp. 2132-2149

6. E. J. Holm and H. P. Langtangen (1999) A unified finite element model for the injection molding process, *Computer Meth. Appl. Mech. Eng.*, Vol.178, pp. 413-429
7. R. Sudduth, Q. Sheng, P. K. Yarala and R. Dugyala (2000) Measurement and computer simulation of crystallinity in injection molded syndiotactic polystyrene, *Proc. SCC 2000*, University of Southern Mississippi, Hattiesburg, MS
8. Q. Sheng, F. F. Farshad and S. Duan (1999) A simulation of crystallinity gradients developed in slowly crystallizing injection molded polymers via parallel splitting, *Eng. Comput.*, Vol.16, pp. 892-912
9. C-M Hsiung and Q. Sheng (1997) A rectilinear flow model approach to the simulation of injection molding process, *J. Reinforced Plastics & Composites*, Vol.16, pp. 1242-1251
10. Y-W Yu and T-J Liu (1999) A hybrid 3D/2D finite element technique for polymer processing operations, *Polymer Eng. Sci.*, Vol.39, pp. 44-54
11. J-F Hetu, D. M. Gao, Garcia-Rejon and G. Salloum (1998) 3D finite element method for the simulation of filling stage in injection molding, *Polymer Eng. Science*, Vol.38
12. G. A. A. Haagh and F. N. Van DeVosse (1998) Simulation of three-dimensional polymer mould filling processes using a pseudo-concentration method, *Inter. J. Numer. Meth. In Fluids*, Vol.28, pp. 1355-1369
13. R. D. Sudduth, P. K. Yarala and Q. Sheng (2001) A comparison of induction time and crystallization rate for syndiotactic polystyrene, accepted for publication in *Polymer Eng. Sci.*
14. R. D. Sudduth, R. Dugyala, Q. Sheng, K. Nichols, and J. Garber (2001) Computer simulation of syndiotactic polystyrene crystallization during injection molding, submitted for publication.
15. C-M Hsiung (1990) *Processing-Structure-Property Relationship and Simulation of Structure gradients in Injection Molded Semi-crystalline Aromatic Polycondensates*, PHD Thesis, University of Akron
16. T. W. Haas and B. Maxwell (1969) *Polymer Eng. Sci.*, Vol.9, pp. 225
17. W. L. Sifleet, N. Dinos and J. R. Collier (1973) Unsteady-state heat transfer in a crystallizing polymer, *Polymer Eng. Sci.*, Vol.13, pp. 10-16
18. J. E. Spruiell and J. White (1975) Structure development during polymer processing: studies of the melt spinning of polyethylene and polypropylene fiber, *Polymer Eng. Sci.*, Vol.15, pp. 660-667
19. R. R. Lagasse and B. Maxwell (1976) An experimental study of the kinetics of polymer crystallization during shear flow, *Polymer Eng. Sci.*, Vol.16, pp. 189-199
20. M. C. Chien and R. A. Weiss (1988) Strain-induced crystallization behavior of poly (Ether-Ether Ketone), *PEEK*, Vol.28, pp. 6-12
21. M. M. Cross (1979) *Rheol. Acta*, Vol.18, pp. 609
22. O. Verhoyen and F. Dupret (1998) A simplified method for introducing the cross viscosity law in the numerical simulation of Hele-Shaw flow, *J. Non-Newtonian Fluid Mech.*, Vol.74, pp. 25-46
23. Q. Sheng , (1989) Solving partial differential equations by exponential splitting, *IMA J. Numer. Anal.*, Vol.9, pp. 199-212

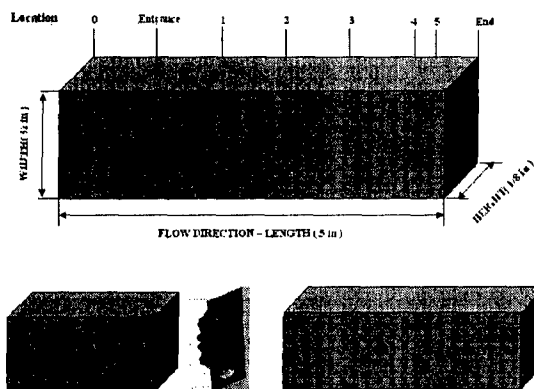


Figure 1 Schematic of Simulated Flex Bar with Locations for Analysis of Cross Sections

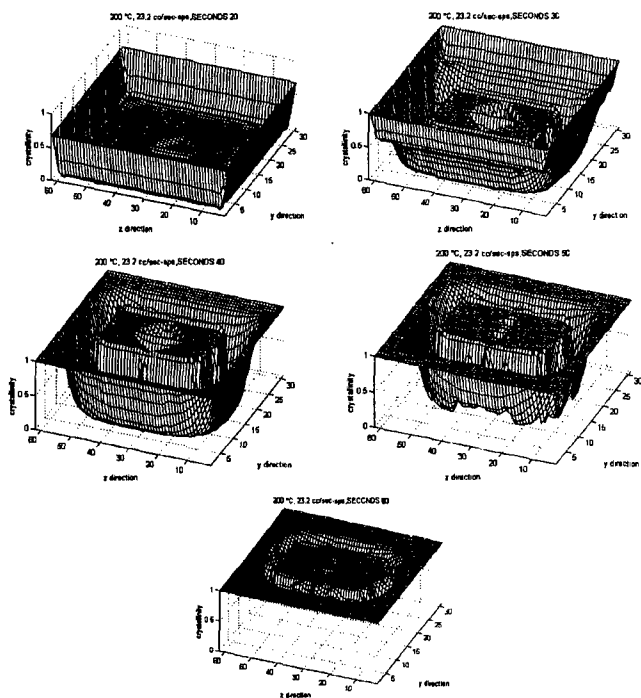


Figure 2 Crystallinity Distributions at a Mold Temperature of 200°C and Different Mold Times at Location#1

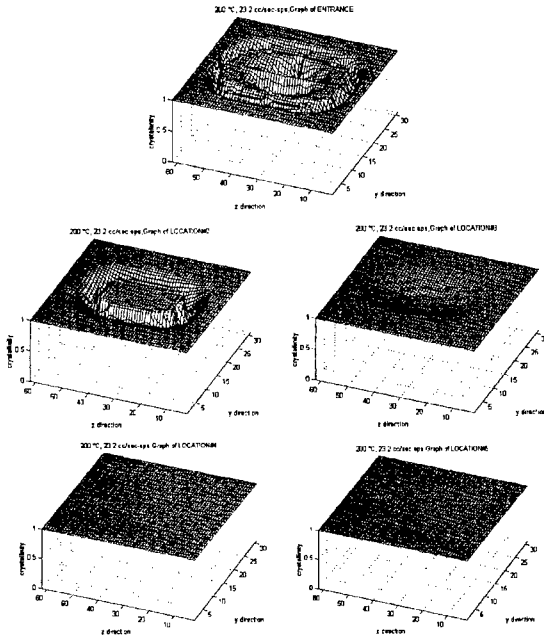


Figure 3 Crystallinity Distribution at Different Locations at a 200°C Mold Temperature after a Hold Time of 60 Seconds

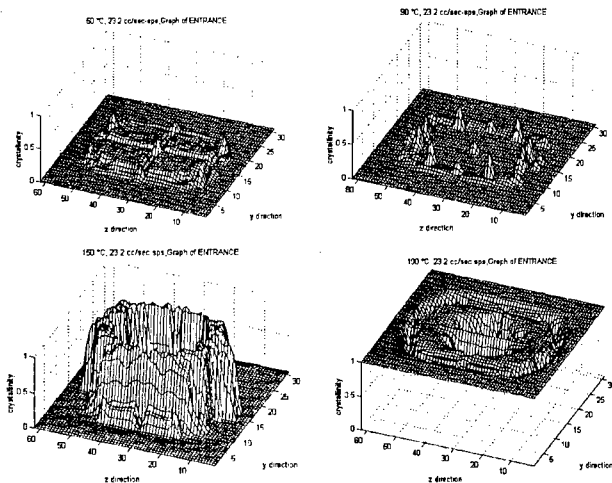


Figure 4 Crystallinity Distributions at the Entrance Location at Four Different Mold Temperatures (50°C, 90°C, 150°C, 190°C)(Injection Speed of 23.2 cc/sec and a Hold Time of 60 sec)

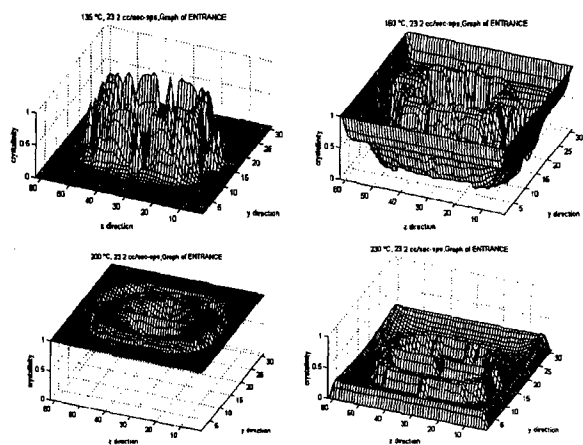


Figure 5 Crystallinity Distributions at the Entrance Location at Four Effective Mold Temperatures (135°C, 160°C, 200°C, 230°C) (Injection Speed of 23.2 cc/sec and a Hold Time of 60 sec)

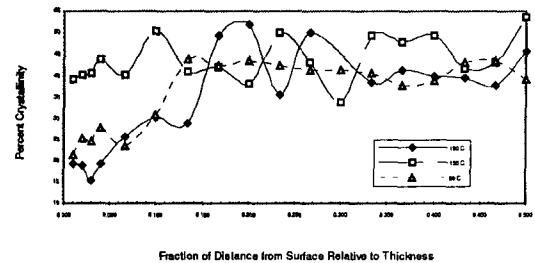


Figure 6 Percent Crystallinity vs Distance from the Surface at Entrance Location for Three Mold Temperatures (90°C, 150°C, 190°C)

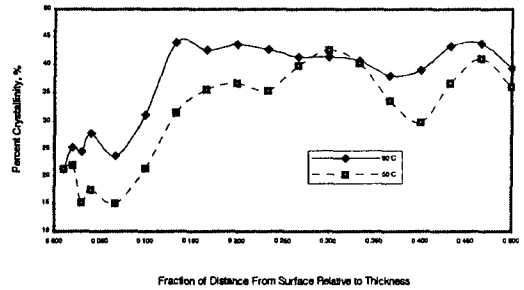


Figure 7 Percent Crystallinity vs Distance from the Surface at Entrance Location and Two Mold Temperatures (50°C, 90°C)